Effect of powder characteristics on tensile properties of additively manufactured 17-4 PH stainless steel

Arun Poudel, Arash Soltani-Tehrani, Shuai Shao, Nima Shamsaei*

National Center for Additive Manufacturing Excellence (NCAME), Auburn University, Auburn, AL 36849, USA

Department of Mechanical Engineering, Auburn University, Auburn, AL 36849, USA

* Corresponding author: shamsaei@auburn.edu

Abstract

Laser beam powder bed fusion (LB-PBF) process uses metallic powders as feedstock, whose particle characteristics such as cohesion, compressibility, size distribution, etc., can vary and affect the mechanical performance of the fabricated parts. In this study, two powder batches of 17-4 precipitation hardening (PH) stainless steel (SS) supplied by EOS (Batch 1) and Carpenter Technology (Batch 2) were used to fabricate specimens using identical process parameters to understand the effects of particle characteristics on defect content as well as tensile performance of the LB-PBF specimens. Higher cohesion and compressibility as well as lower sphericity in Batch 2 resulted in specimens with higher porosity levels. During tensile testing, the higher porosity level in Batch 2 yielded lower ductility. In contrast, the microstructure was observed to be less sensitive to particle characteristics because of which the tensile strengths of the specimens were found to be comparable to each other.

KEYWORDS: Additive manufacturing, Tensile performance, Powder characteristics, Powder flowability, Porosity, LB-PBF

Introduction

One of the common techniques to generate powder is gas atomization, and the output can be used in powder-based additive manufacturing (AM) technologies such as laser or electron beam powder bed fusion (LB- or EB-PBF) [1]. Therefore, the rheological behavior of the gas-atomized powders such as their flowability, spreadability, and packing density can influence the mechanical performance of the resulting parts. Powder rheological behavior is itself affected by many factors including but not limited to particle size distribution (PSD), cohesion, internal porosity, and sphericity of the powder particles. Studies attempting to understand the influence of these powder characteristics on the mechanical performances of the additively manufactured (AMed) parts are relatively limited [2–4].

Powder characteristics such as sphericity and PSD are a few of the most influential characteristics of powder flowability. Higher sphericity, as well as fewer satellites (i.e., smaller powder particles being attached to the bigger ones [5]), can typically result in higher flowability and consequently denser LB-PBF parts [4,6,7]. Muniz-Lerma et al. [8] also reported that a wider PSD can result in more agglomerates and higher cohesion between the powder particles and

ultimately less dense materials. Similar observations were reported by Simchi [9] that the existence of very fine and coarse/large particles within the powder batch (i.e. a wider PSD) can adversely affect the part density. The reason was explained by the tendency of fine particles to agglomerate and large particles to segregate.

Comparable observations were also reported by Carrion et al. [10] and Soltani-Tehrani et al. [11]. In these studies, the narrower PSD which included the particles with more uniform sizes was seen to result in not only a higher powder flowability but also a higher packing density. It was detailed that the existence of agglomerates within the batch can lead to more empty spaces within the powder bulk. These empty spaces were reported to negatively influence the consolidation of the powder layers to the previously solidified layers during the LB-PBF process. As a result, more pores with larger sizes were observed in the LB-PBF parts fabricated from powder batches with wider PSDs.

Although it is well established that particle morphology and PSD can affect powder behavior and consequently mechanical properties, limited research studies have correlated such variations in powder with the AMed part performance. As a result, this study aims to provide some insights into the relationships between the powder feedstock and structure-part performance. It is also noteworthy to mention that America Makes and the American National Standards Institute (ANSI) have reported the "*flowability*", "*spreadability*", "*particle size and particle size distribution*", "*particle morphology*", "*hollow particles and hollow particles with entrapped gas*", and "*metal powder specifications*" as some major technical gaps (PM1, 4, 6, and 7) in the additive manufacturing standardization collaborative (AMSC) roadmap [12], necessitating more in-depth investigations and further research.

Material and methods

Two different batches of argon atomized 17-4 PH stainless steel (SS) powder supplied by EOS (Batch 1) and Carpenter Technology (Batch 2) were used to fabricate some cylindrical bars with an 11 mm diameter and 84 mm length using identical process parameters in the EOS M290 LB-PBF AM machine. The chemical composition of each of the powder batches, reported by the manufacturer, is shown in **Table 1**. EOS has reported the chemical composition of its powder following the ASTM F899 standard. After fabrication, the cylindrical bars were subjected to the CA-H1025 heat treatment procedure (i.e. solution annealing at 1050 °C for ½ hour followed by air cooling and aging at 552 °C for 4 hours and the subsequent air cooling) to homogenize and strengthen the microstructure [13]. Finally, the heat-treated specimens were machined into the net-shape fatigue specimens with tangentially blending fillets between the test section and the ends following ASTM E466 for uniaxial force-controlled fatigue testing [14]. The tensile tests were performed using the fatigue specimens on an MTS servo-hydraulic load frame with a 25 KN load cell according to ASTM E8 standards [15].
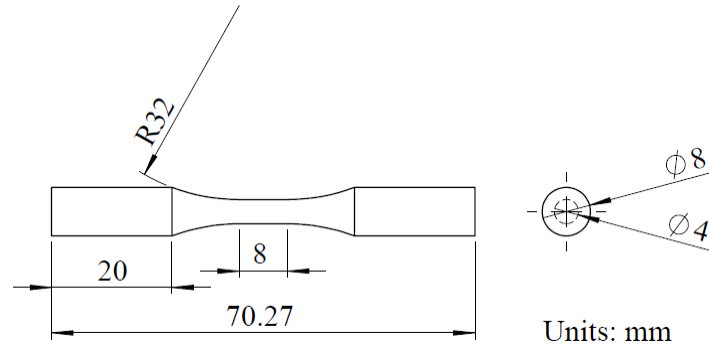
Fig. 1. The geometry of the machined specimens following ASTM E466 standards [16].

Table 1 Chemical composition of the 17-4 PH SS powder reported by the powder's manufacturers (i.e., Batch 1 from EOS and Batch 2 from Carpenter technology).

| Element (Wt. %)	Batch 1	Batch 2
C	0.010	0.010
Cr	16.300	16.670
Ni	4.180	4.270
Cu	4.100	3.680
Mn	0.220	0.050
Si	0.400	0.020
Nb	0.250	0.310
Mo	0.020	0.080
N	0.040	0.100
O	0.050	0.030
P	0.012	0.010
S	0.004	0.004
Fe	Bal.	Bal.

Powder characteristics such as compressibility, cohesion, bulk and tapped densities, and shear stress (according to ASTM D7891 [17]) of both powder batches were investigated using Freeman Technology (FT4) powder rheometer. Furthermore, the PSD was analyzed as per ASTM E2651 standard [18] using an Anton Paar PSA 1190 with laser diffraction technology. The internal porosity of the powders particles and their morphology was studied using a Zeiss Xradia 620 Versa, an X-ray computed tomography (CT) machine and a Zeiss Crossbeam 550 SEM/FIB scanning electron microscope (SEM), respectively. In addition, the porosity content in the fabricated specimens was studied and quantified on polished cross sections by using Keyence VHX-6000 digital optical microscope.

Results and discussion

Powder characteristics

Different characteristics of the powder such as its flowability, spreadability, packing density can influence the part performances. Even though the parameters such as flowability and

spreadability represent the powder flow throughout the build plate, they can also have a major influence on the porosity formation of the resulting AM parts. As seen in **Figs. 2** (a & b), the powder particles' morphology illustrated the existence of both spherical particles and agglomerates in both powder batches. However, visually comparing both batches, Batch 2 seems to consist of particles with relatively high sphericity as can be seen in **Fig. 2**(b) while the particles in Batch 1 have more irregularly-shaped particles (see **Fig. 2**(a)). In addition, comparing the SEM images, Batch 1 had a higher level of open porosity in the powder particles as compared to Batch 2. The analysis performed using SEM agrees with the findings from the X-ray CT scanning of the powders in **Figs. 2** (c & d). As seen in these figures, the level of internal porosity (colored in red) in the Batch 1 powder particles is higher than in Batch 2. Some studies have reported that the existence of internal particle porosity contributes to the gas entrapment and less dense LB-PBF fabricated parts [2,19,20].
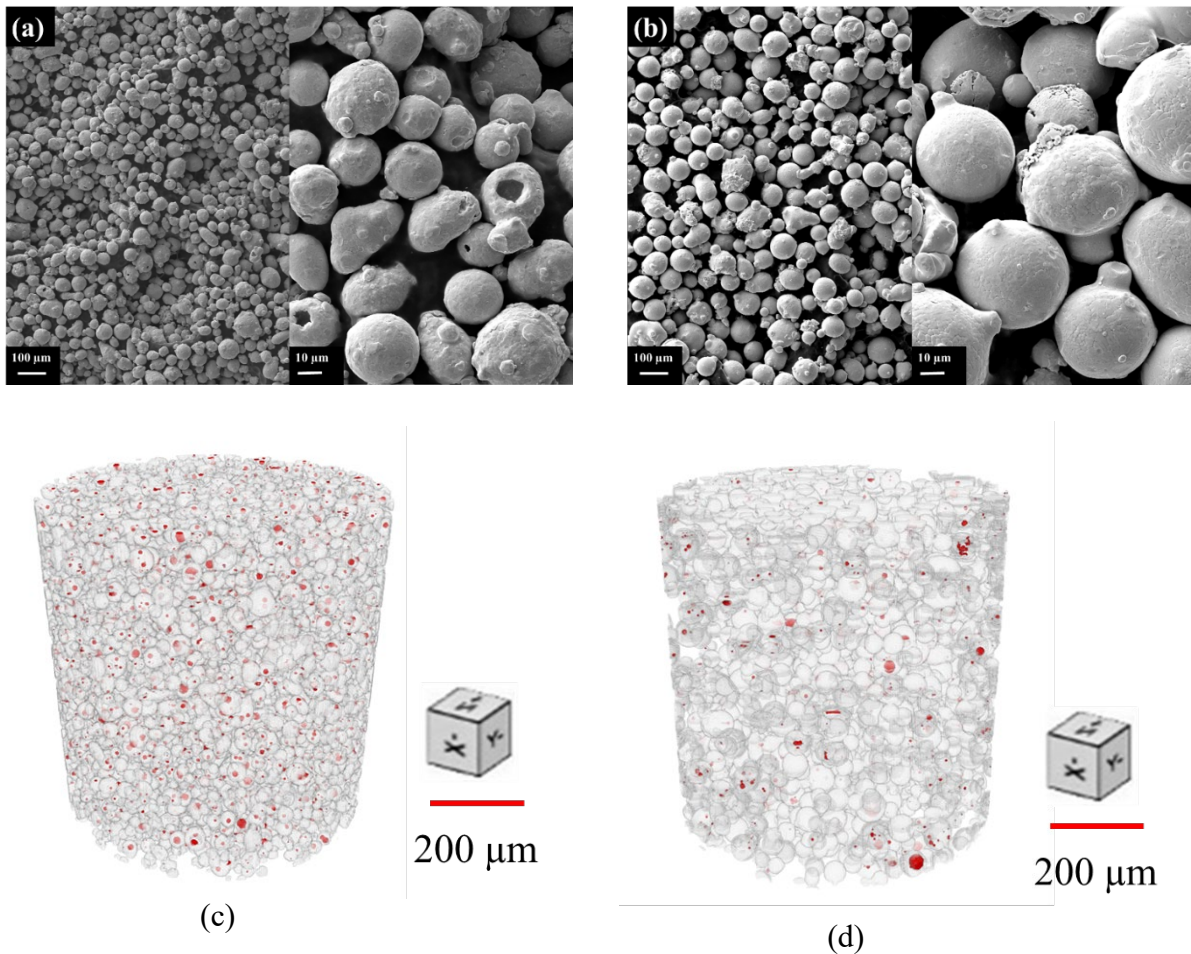

Fig. 2. Morphology of (a) Batch 1, and (b) Batch 2 17-4 PH SS powder particles obtained via Zeiss Crossbeam 550 SEM, and X-ray CT 3D visualizations of (c) Batch 1 and (b) Batch 2 powders illustrating internal porosities and morphology.

Also, in **Fig. 3**(a), the PSD of both powder batches illustrates a clear difference in the mean particle diameter and also the existence of finer particles in Batch 1. The mean particle size of Batch 2 was observed to be 49 µm which is 40% larger than that of Batch 1. Similarly, the D_{10} and

D$_{90}$ of the Batch 1 powder was found to be 22 µm and 47 µm whereas for Batch 2, it was 30 µm and 65 µm respectively. Therefore, it can be distinctly concluded that more fine particles exist in Batch 1. Fine powder particles have been observed to decrease the powder flowability and resulting in inferior powder spreadability on the build plate during fabrication due to higher interparticle friction [21,22].

This observation also supports the finding regarding the densities of powder particles in both apparent and tapped conditions. The Hausner ratio (i.e., the ratio of tapped to apparent powder density) of Batch 1 and 2 was found to be 1.08 and 1.04, respectively. Both apparent and tapped densities were observed to be lower in Batch 1 because of the higher internal porosity and tendency to form agglomerates. The non-uniform packing state caused by the formation of the agglomerates can result in a higher percentage of compressibility due to more void spaces among particles, and also higher cohesion (see **Fig. 3** (c & d)). The higher cohesion in Batch1 due to the presence of more fine particles can hinder the powder flow and its uniform spreadability across the build plate [8].
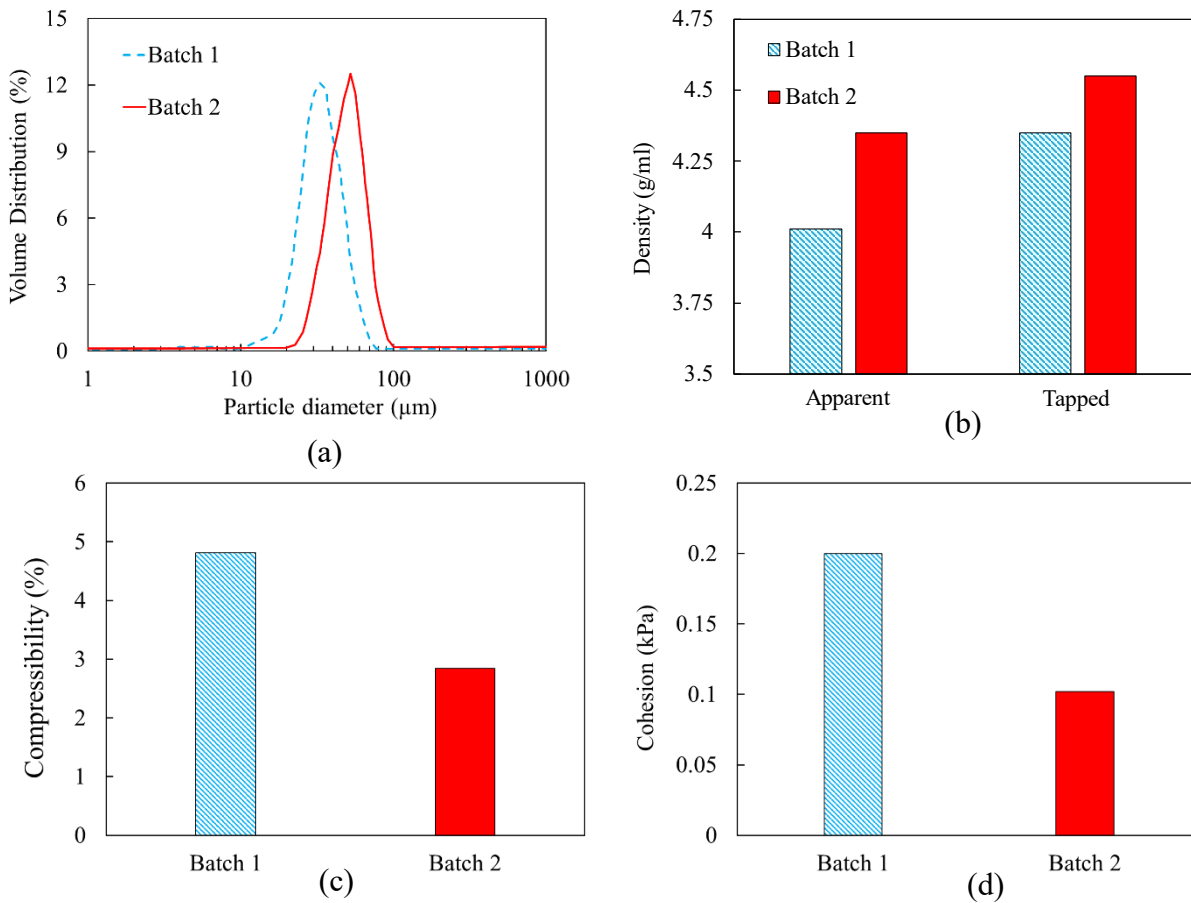
Fig. 3. Comparison of the 17-4 PH SS powders' characteristics: (a) PSD, (b) apparent and tapped densities, (c) compressibility, and (d) cohesion.

Porosity level of fabricated parts

Porosity analysis of the specimens fabricated using Batches 1 and 2 powders with their corresponding pore size distribution and its standard deviations between 4 layers is shown in **Fig. 4**. It seems that the specimens fabricated using Batch 2 powder have a lower porosity level. This behavior was also consistent with the rheological findings where Batch 2 was observed to have a higher flowability and superior packing state due to lower cohesivity, narrower PSD, less internal particle porosity, and higher sphericity. In addition, the standard deviation in the porosity count in the specimen fabricated using Batch 2 powder is much lower as compared to Batch 1 in all porosity size ranges which can suggest the consistency in the porosity distribution between consecutive layers. Similar findings have been reported in Ref. [2] where the powder with finer particles resulted in more agglomerates, a non-uniform powder distribution, and less dense materials.
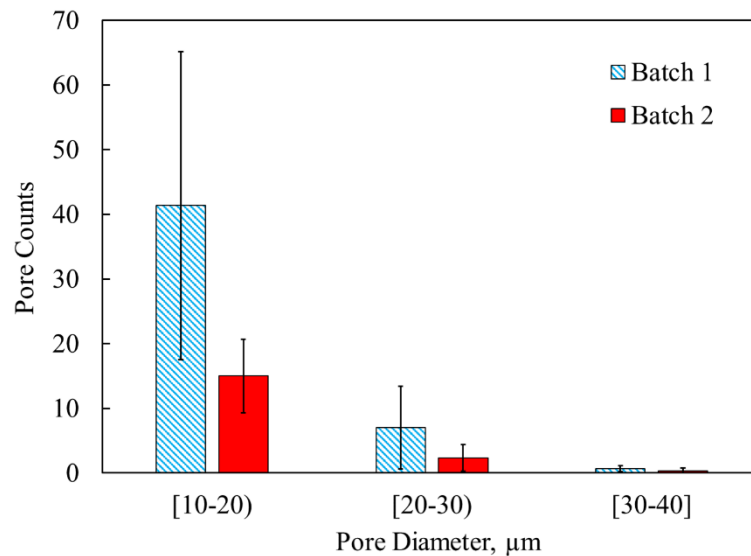

Fig. 4. Comparison between the porosity levels of LB-PBF 17-4 PH SS specimens fabricated from Batches 1 and 2.

Tensile properties

The quasi-static tensile behaviors of LB-PBF 17-4 PH SS parts fabricated from Batch 1 and 2 are presented in **Fig. 5**. The ultimate tensile strength (UTS) and yield strength (YS) of Batch 1 specimens were slightly higher than Batch 2 (~7%). This small difference in tensile strength can be attributed to the different powder densities. As noted in **Fig. 3(b)**, the bulk density of Batch 2 was 8.5% higher than Batch 1. Typically, powder batches with smaller particle sizes should have better thermal contact and better thermal conductivity. Therefore, it can be assumed that the higher thermal conductivity of Batch 1 has resulted in more heat dissipation toward the build plate, higher temperature gradient in the part, and consequently higher cooling rates during fabrication. As a result, the grains are expected to be somewhat larger in Batch 2 specimens [23,24]. Similar values of UTS and YS were also reported by Nezhadfar et al. [25] for 17-4 PH SS material subjected to CA-H1025 heat-treatment process. In terms of ductility, the strain to fracture (ε_f) for Batch 2 was observed to be 8.6% higher than Batch 1. Since the defect content in the specimens can influence the ductility of the materials, the lower porosity level in Batch 2 should have contributed to its

superior ductility. Similar observations were reported in Ref. [4], where a lower ductility was correlated with higher porosity resulted from lower flowability as well as more fine particles within the batch. The comparison of the tensile properties of the 17-4 PH SS material obtained in this study with the ones in the literature can be seen in **Table 2**.
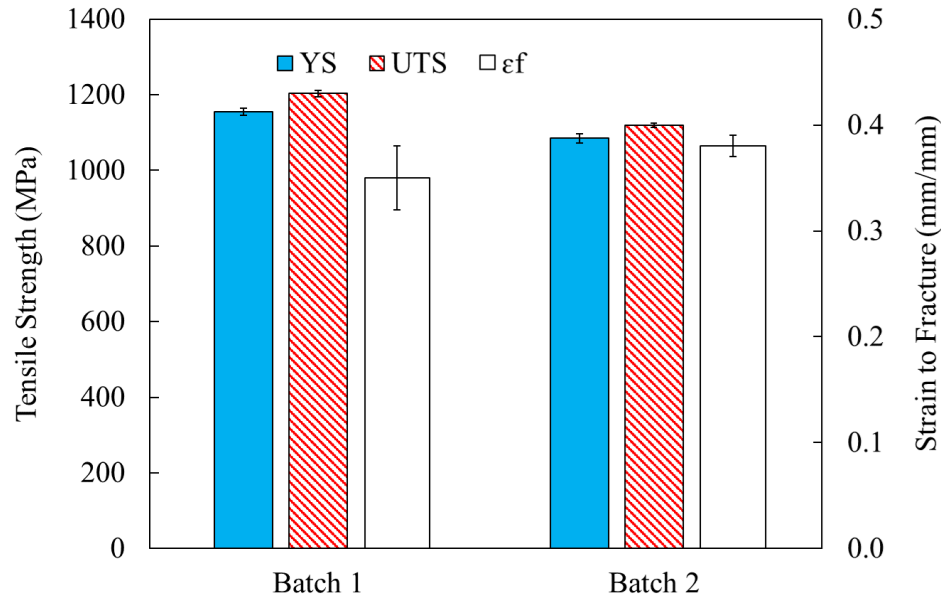
Fig. 5. Comparison between the UTS, YS and ε_f of the LB-PBF 17-4 PH SS specimens fabricated using Batch 1 and 2 powders.

Table 2 Comparison of tensile strengths obtained in this study with the ones from the literature.

17-4 PH SS	Heat Treatment	UTS (MPa)	YS (MPa)	Strain to fracture (mm/mm)
Batch 1	CA-H1025	1203	1155	0.35
Batch 2	CA-H1025	1119	1085	0.38
Nezhadfar et al. [25]	CA-H1025	1167	1140	0.30
Carpenter Technology [26]	H950	1172	1069	N/A
Wrought (EOS) [27]	CA-H900	1336	1235	N/A

Conclusions

The powder characteristics such as compressibility, cohesion, morphology, PSD, etc. were observed to influence the porosity as well as the mechanical properties of the AMed 17-4 PH SS parts.

- Higher compressibility, cohesion, and the presence of more irregularly shaped and fine particles in Batch 1 resulted in higher porosities.
- Ductility was lower in the Batch 1 specimens due to the higher level of porosity.

- As opposed to ductility, the tensile strength was observed to be less sensitive to the variations in powder properties.

Acknowledgments

References

[1]   P. Moghimian, T. Poirié, M. Habibnejad-Korayem, J.A. Zavala, J. Kroeger, F. Marion, F. Larouche, Metal powders in additive manufacturing: A review on reusability and recyclability of common titanium, nickel and aluminum alloys, Addit. Manuf. 43 (2021) 102017. https://doi.org/10.1016/j.addma.2021.102017.

[2]   A.T. Sutton, C.S. Kriewall, M.C. Leu, J.W. Newkirk, Powder characterisation techniques and effects of powder characteristics on part properties in powder-bed fusion processes, Virtual Phys. Prototyp. 12 (2017) 3–29. https://doi.org/10.1080/17452759.2016.1250605.

[3]   B. Liu, R. Wildman, C. Tuck, I. Ashcroft, R. Hague, Investigaztion the effect of particle size distribution on processing parameters optimisation in selective laser melting process, 22nd Annu. Int. Solid Free. Fabr. Symp. - An Addit. Manuf. Conf. SFF 2011. (2011) 227–238.

[4]   A. Strondl, O. Lyckfeldt, H. Brodin, U. Ackelid, Characterization and Control of Powder Properties for Additive Manufacturing, Jom. 67 (2015) 549–554. https://doi.org/10.1007/s11837-015-1304-0.

[5]   Anti-Satelliting for Powders Produced Inert Gas Atomisation, (n.d.). https://www.azom.com/article.aspx?ArticleID=1541 (accessed June 9, 2021).

[6]   V. V. Popov, A. Katz-Demyanetz, A. Garkun, M. Bamberger, The effect of powder recycling on the mechanical properties and microstructure of electron beam melted Ti-6Al-4V specimens, Addit. Manuf. 22 (2018) 834–843. https://doi.org/10.1016/j.addma.2018.06.003.

[7]   H.P. Tang, M. Qian, N. Liu, X.Z. Zhang, G.Y. Yang, J. Wang, Effect of Powder Reuse Times on Additive Manufacturing of Ti-6Al-4V by Selective Electron Beam Melting, Jom. 67 (2015) 555–563. https://doi.org/10.1007/s11837-015-1300-4.

[8]   J. Muñiz-Lerma, A. Nommeots-Nomm, K. Waters, M. Brochu, A Comprehensive Approach to Powder Feedstock Characterization for Powder Bed Fusion Additive Manufacturing: A Case Study on AlSi7Mg, Materials (Basel). 11 (2018) 2386. https://doi.org/10.3390/ma11122386.

[9]   A. Simchi, The role of particle size on the laser sintering of iron powder, Metall. Mater. Trans. B Process Metall. Mater. Process. Sci. 35 (2004) 937–948. https://doi.org/10.1007/s11663-004-0088-3.

[10]   P.E. Carrion, A. Soltani-Tehrani, N. Phan, N. Shamsaei, Powder Recycling Effects on the Tensile and Fatigue Behavior of Additively Manufactured Ti-6Al-4V Parts, Jom. 71 (2019) 963–973. https://doi.org/10.1007/s11837-018-3248-7.

[11]   A. Soltani-Tehrani, J. Pegues, N. Shamsaei, Powder recycling of 17-4 PH SS, Addit. Manuf. (2020).

[12]   America Makes, AMSC, Standardization Roadmap for Additive Manufacturing, 2018.

[13]   P.D. Nezhadfar, R. Shrestha, N. Phan, N. Shamsaei, Fatigue behavior of additively manufactured 17-4 PH stainless steel: Synergistic effects of surface roughness and heat

treatment, Int. J. Fatigue. 124 (2019) 188–204. https://doi.org/10.1016/j.ijfatigue.2019.02.039.

[14] ASTM, Standard Practice for Conducting Force Controlled Constant Amplitude Axial Fatigue Tests of Metallic Materials, Test. 03 (2002) 4–8. https://doi.org/10.1520/E0466-07.2.

[15] Standard Test Methods for Tension Testing of Metallic Materials 1, (n.d.). https://doi.org/10.1520/E0008_E0008M-16AE01.

[16] ASTM Compass, (n.d.). https://compass.astm.org/EDIT/html_annot.cgi?E466+15 (accessed June 9, 2021).

[17] American Society for Testing Material, Standard test method for shear testing of powders using the freeman technology FT4 powder rheometer shear cell, Astm D7891-15. (2015) 1–11. https://doi.org/10.1520/D7891-15.1.5.

[18] T. Allen, Particle Size Measurement, Springer Netherlands, Dordrecht, 1990. https://doi.org/10.1007/978-94-009-0417-0.

[19] M. Iebba, A. Astarita, D. Mistretta, I. Colonna, M. Liberini, F. Scherillo, C. Pirozzi, R. Borrelli, S. Franchitti, A. Squillace, Influence of Powder Characteristics on Formation of Porosity in Additive Manufacturing of Ti-6Al-4V Components, J. Mater. Eng. Perform. 26 (2017) 4138–4147. https://doi.org/10.1007/s11665-017-2796-2.

[20] S.M.H. Hojjatzadeh, N.D. Parab, Q. Guo, M. Qu, L. Xiong, C. Zhao, L.I. Escano, K. Fezzaa, W. Everhart, T. Sun, L. Chen, Direct observation of pore formation mechanisms during LPBF additive manufacturing process and high energy density laser welding, Int. J. Mach. Tools Manuf. 153 (2020) 103555. https://doi.org/10.1016/j.ijmachtools.2020.103555.

[21] W. Wle, An overview of powder granulometry on feedstock and part performance in the selective laser melting process, (2017). https://doi.org/10.1016/j.addma.2017.10.011.

[22] S.E. Brika, M. Letenneur, C.A. Dion, V. Brailovski, Influence of particle morphology and size distribution on the powder flowability and laser powder bed fusion manufacturability of Ti-6Al-4V alloy, Addit. Manuf. 31 (2020) 100929. https://doi.org/10.1016/j.addma.2019.100929.

[23] C. Gao, K. Kuklane, I. Holmér, Cooling vests with phase change material packs: The effects of temperature gradient, mass and covering area, Ergonomics. 53 (2010) 716–723. https://doi.org/10.1080/00140130903581649.

[24] N. Raghavan, R. Dehoff, S. Pannala, S. Simunovic, M. Kirka, J. Turner, N. Carlson, S.S. Babu, Numerical modeling of heat-transfer and the influence of process parameters on tailoring the grain morphology of IN718 in electron beam additive manufacturing, Acta Mater. 112 (2016) 303–314. https://doi.org/10.1016/j.actamat.2016.03.063.

[25] P.D. Nezhadfar, R. Shrestha, N. Phan, N. Shamsaei, Fatigue behavior of additively manufactured 17-4 PH stainless steel: Synergistic effects of surface roughness and heat treatment, Int. J. Fatigue. 124 (2019) 188–204. https://doi.org/10.1016/j.ijfatigue.2019.02.039.

[26] Carpenter Technology, 17-4 PH stainless steel, (n.d.).

[27] E. GmbH, EOS StainlessSteel 17-4PH, (n.d.).